Strain analysis of a glass-fibre-reinforced polyester under dynamic loads

A. Silvera[1]*, J. Vazquez[2] and V. Vinssac[1]

[1] Departamento de Ingeniería Rural. Escuela Universitaria de Ingeniería Técnica Agrícola.
Universidad Politécnica de Madrid. Ciudad Universitaria. Madrid. Spain
[2] Departamento de Ingeniería Rural. Escuela Técnica Superior de Ingenieros Agrónomos.
Universidad Politécnica de Madrid. Ciudad Universitaria. Madrid. Spain

Abstract

Strain on fibreglass-reinforced polyester was analysed for different types of stress-strain patterns to determine the existence of a critical point on the respective diagrams. This critical point defines the maximum strain value prior to a steep and abrupt increase that causes failure. «Useful life» should, therefore, be regarded to be the number of cycles associated with the critical point rather than the number associated with failure. The tests conducted in this study showed that the number of critical point cycles was around 95% of the yield point cycles. The degradation rate of the material tested under different loads was found with an analytical model applied to the most common strain pattern. The model proposed also showed that the stress ratio, R, was related to elastic modulus degradation. When studied for load state values of 10 to 16% of the ultimate tensile strength (UTS), material life expectancy was found to be 10^4 to 10^7 cycles. No fatigue limit appeared for these values, however. Immersion of the material in water and subsequent drying under ambient conditions was found not affecting either deformation or deformation-related variables. Finally, a model was developed to predict life expectancy from the maximum strain values.

Additional key words: admissible strain; composite; degradation; elastic modulus; fatigue; glass fibre reinforced polyester; useful life; wind turbine blades.

Resumen

Estudio de la deformación de un material compuesto de fibra de vidrio y resina de poliéster sometido a cargas dinámicas

En esta investigación se plantea el análisis del proceso de deformación por fatiga del material compuesto bajo diferentes condiciones de carga cíclica y amplitud constante durante todo el proceso. También se ha analizado la influencia de la humedad en el proceso de deformación. La metodología de trabajo seguida se ha basado en la realización de ensayos destructivos (método de fatiga) y el seguimiento de los mismos utilizando un captador de deformaciones y un software específico. El proceso de degradación ha dado lugar a diferentes tipologías del diagrama de deformación y a la observación de un punto crítico en ese diagrama. Ese punto ha permitido establecer un valor límite para la deformación (deformación admisible) y otro valor límite para la vida sin riesgo de rotura (vida útil). Se ha hallado una esperanza de vida del material del orden de 10^4 a 10^7 ciclos, para valores de la carga máxima en fatiga comprendidos entre el 10% y el 16% de la tensión de rotura, no apareciendo, a estos niveles, indicio alguno de un posible límite de rotura. Se ha aplicado un modelo de análisis a la tipología de deformación más común hallada, que permite cuantificar la tendencia a la degradación en las distintas condiciones de carga y de humedad ensayados.

Palabras clave adicionales: deformación; degradación; fatiga; materiales compuestos; módulo elástico; poliéster reforzado con fibra de vidrio; vida útil.

Introduction

To ensure the durability of structural parts, designers must have a full working knowledge of the properties of the materials used (Andersen *et al.*, 1988; Bach, 1992, 1994), under both static and dynamic conditions. At the same time, safety factors must be built into the design to accommodate uncertainties associated both with the material itself and the environmental conditions to which it will be exposed.

The general objective of fatigue tests is to predict the life expectancy of structural parts. Many models are in place to calculate the expected number of cycles that can be withstood by a material, based on S-N curves. Andersen *et al.* (1988) and Bach (1988, 1991) reported that the fatigue life of a material can be predicted with an equation proposed by Mandell (1982) that relates the applied stress to the number of cycles:

$$\sigma = \sigma_U (1 - y_0 \log N) \qquad [1]$$

where σ (MPa) is the applied stress; σ_U the ultimate tensile strength (MPa), N the number of cycles and y_0 a coefficient dependent on the stress ratio R and the type of material.

Vázquez *et al.* (1998) developed a model to predict the expected number of cycles based on fatigue test data for different values of R. Their model is as follows:

$$\text{Number of cycles} = a \, x^b \qquad [2]$$

where *a, b* are generic statistical coefficients; *x* is the modified variable σ_U/σ_{max}; σ_U is ultimate tensile strength (UTS) (MPa); and σ_{max} is the maximum stress applied (MPa).

According to Reifsnider (1991), when strength falls below a certain value, the useful life of the member in question is regarded to be over. Behaviour models based on a large number of tests provide a clearer view of these developments, which have been studied by Yang *et al.* (1983), Reifsnider (1991) and Oller (2002), among others. Their techniques call for destructive testing, however, in which degradation is difficult to monitor.

A number of studies by O'Brien (1985) and Talreja (1986, 1997), for instance, relate the variation in material stiffness to the density of cracks in the matrix and the extent of scaling. Paris *et al.* (1961) proposed a mathematical relationship between the useful life of a material and crack length.

Hwang and Han (1986) introduced a simple model using the fatigue modulus concept, which establishes a relationship between the force applied and the deformation generated in the laminate for a given number of fatigue cycles. The material fails when the deformation induced reaches a threshold, expressed in per cent of the ultimate static deformation.

Several researchers have defined a so-called «damage variable». Reifsnider (1991), for instance, proposed a damage variable defined as D = (Sn-Sr)/(Sn-S) (where Sn is the static strength, Sr the residual strength and S the test stress applied). When D = 0, Sn = Sr, in which case the material undergoes no degradation, and when D = 1 the residual strength equals the existing strength.

Bach (1994), in turn, related the expected number of cycles to the variable d = E/E$_0$ (where E is present and E$_0$ initial stiffness). His findings showed that the number of useful life fatigue cycles was 70% of the number of cycles needed to induce failure.

Anderson (1996) established the following ratio: $100(\varepsilon/\varepsilon_{max})$, where ε_{max} is the strain prior to failure (ε_C in this paper).

The present study aimed to assess the behaviour of fibreglass-reinforced polyester (GFRP) under static and dynamic loading. The specific objectives pursued were: i) to calculate the expected number of fatigue cycles withstood by the material from the S-N diagram; ii) to study the strain diagram and observe possible variations under different load states; iii) to identify the possible existence of a critical point on the strain diagram that would be indicative of impending material failure, and to establish the strain limit values; iv) to study the effect of the stress ratio, R, on material deformation; and v) to study how deformation is affected by the intensity of moisture absorption-induced ageing.

Material and methods

The tests were conducted on a 50-kN Amsler 50 PZBDA 401 hydraulic testing frame suitable for both static and dynamic trials. The minimum load in dynamic trials was set at 7 kN, due to apparatus instability under that value. The pulse frequency used in the short duration trials was 4.16 Hz (250 pulses min^{-1}). In the long duration trials, however, pulse frequency was raised to 8.33 Hz (500 pulses min^{-1}), for the sole purpose of shortening testing time. Frequency does not affect fatigue strength in this range.

Fibre layout in the samples is shown in Figure 1. Each sample had 15 one-directional laminates with a density of 500 g m^{-2} and four cross-ply laminates (at $\pm 45°$), interspersed after every fifth one-dimensional laminate, with a density of 300 g m^{-2}.

Fibre characteristics were as follows: RO 99P-177 1200 tex, direct D, type E wire; mass (ISO-1889) = 1,200 g km^{-1}. The matrix characteristics were: ESTRATIL 2123 polyester; density (UNE 553020) = 1.2 g cm^{-3}; water absorption under ambient conditions (UNE 53028 44 cm^3) = 0.15%; tensile strength (UNE 53023) = 54 MPa.

The estimated volume percentage of fibreglass was 61.97. Test sample dimensions and shapes are shown in Figure 2. All tests were conducted with rectangular rather than the conventional dog-bone specimens because avoiding the size effect was regarded to be crucial in fatigue testing. This led to the use of identical samples in all tests. In addition, given the minimum load accommodated by the testing frame (7 kN) and the grip width, all the specimens were designed as shown in Figure 2.
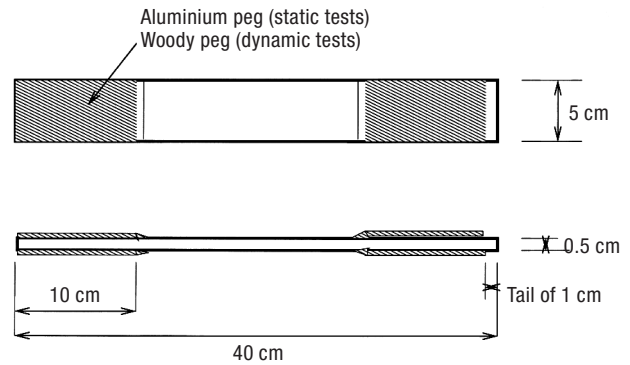
The tails of 23 test samples were burned to find their fibre content, expressed in per cent by volume.

Static tests

Twenty samples of the material were tested for ultimate tensile strength; UTS or σ_U (MPa). The loading
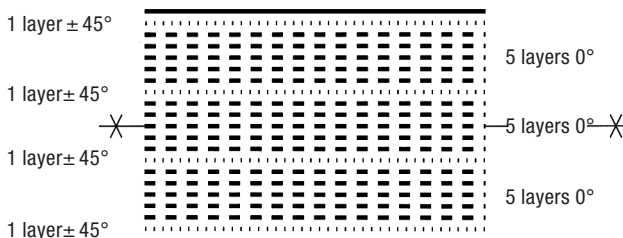
Figure 1. Fibreglass fibre arrangement in test samples: four cross-ply laminates ($\pm 45°$) and 15 one-directional laminates.

Figure 2. Tests sample shapes and dimensions.

rate used, 10 kN min^{-1}, was within the range of values recommended by Greenwood (1981). All the samples were checked to determine the consistency of their fibre content and the possible effect of modifications in that variable on the mechanical properties of the material. Deformation was measured with a linear variable differential transformer (LVDT) connected to a data logger.

The readings were entered in the statistical software to find the cumulative distribution function (CDF) of all the variables studied.

Dynamic tests

The testing frame generated sinusoidal tensile stress, characterised by the minimum (σ_{min}) and maximum (σ_{max}) stress applied and the R = $\sigma_{min}/\sigma_{max}$ ratio.

The load states (σ_{av}/σ_U) 100, which fell within the elastic range of the material, varied from 16% to 10% of the UTS. Deformation was monitored by continuous strain measurements and plotted against the number of fatigue cycles (N_v). The present study introduced a strain factor F_v, the «damage variable», which was related to the life factor G_v, another variable.

Effect of moisture on GFRP

In this paper, three series of test samples exhibiting type I behaviour (see Results, section «Strain analysis and typologies») were subjected to the series B loading conditions. The effect of moisture absorption on deformation was studied by conducting two (2H) or three (3H) wet-dry cycles, consisting in immersion in water at 20°C followed by drying at ambient temperature for varying lengths of time.

Table 1. Mechanical characteristics of the material

	σ_U (MPa)[1]	E (GPa)[2]	σ_p (MPa)[3]	E* (GPa)[4]
CDF[5]	Weibull	Lognormal	Lognormal	Lognormal
β[6]	11.7			
γ[7]	921.3			
μ[8]		60.54	503.6	52.54
λ[9]		7.57	126.88	6.36
K-S[10]	0.82	0.61	0.97	0.76

[1] Ultimate tensile strength (UTS). [2] Elastic modulus. [3] Proportional limit. [4] Slope of the second linear region on the stress-strain diagram. [5] Cumulative distribution function. [6] Shape parameter (Weibull function). [7] Characteristic value (Weibull function). [8] Characteristic value (lognormal function). [9] Shape parameter (lognormal function). [10] Kolmogorov-Smirnov statistic. [10] Cumulative distribution function.

Results

Static tests

Mechanical characteristics of the material

All the samples were fitted to a Weibull function, in which the characteristic value was $\sigma_U = 921.3$ MPa (see Table 1). The σ_p (MPa) values, in turn, were fitted to the lognormal function, where the proportional limit, σ_p, was 503.6 MPa. The most likely value for the elastic modulus, E, was E = 60.54 GPa. The stress/strain diagram confirmed the existence of two distinct linear regions. The E* value, or slope of the second linear region, was 52.54 MPa (Table 1).

Influence of the glass-fibre volume percentage V_f

A statistical analysis of the findings showing that the most likely V_f value was 61.97% also yielded the following results: CDF: Weibull, $\beta = 19.1$, $\gamma = 61.97$ and K-S = 0.99.

Regression analysis based on the values of the elastic modulus and UTS found that while V_f had no effect on σ_U ($R^2 = -0.026$) it was consistently correlated to E ($R^2 = 0.742$).

Dynamic tests

S/N diagram

The S-N diagram (Fig. 3) was plotted with a short number of load states, ranging from 16 to 20% of the UTS, whose respective σ_{max} values were 117.6, 156.8 and 235.2 MPa. As Table 2 shows, the σ_{min} value was 58.8 MPa in all the tests conducted. The S-N diagram was plotted for the entire suite of tests, *i.e.,* 15 each in series A, B and C (Table 2). These data were used to determine the characteristic fatigue life (N) values.

The failure model developed for the maximum stress applied, σ_{max} (MPa), was expressed as:

$$\sigma_{max} = 930.72\ N^{-0.1254} \qquad [3]$$

where N is the number of cycles; the resulting correlation coefficient was $R^2 = 0.9872$.

The model can be fitted to a straight line (see Fig. 3) as follows:

$$\sigma_{max} = -49.91 \log N + 471.74 \qquad [4]$$

Testing a previous model of life prediction

A failure model was developed for a similar GFRP but with lower density (300 gm^{-2}) and a σ_U (660 MPa) values. This failure model was defined as
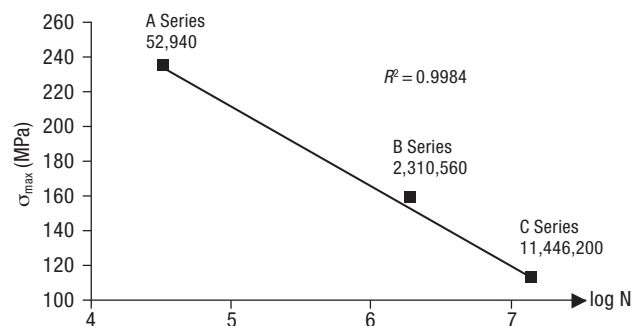
Figure 3. S-N diagram (maximum stress σ_{max} (MPa) *vs.* log of number of cycles (N), for series A, B and C (Table 2). Correlation to real data: $R^2 = 0.9984$.

Table 2. Fatigue load states

Series	σ_{max} (MPa)[1]	Load state (σ_{av}/σ_U) 100	N (cycles)[2]
A	235.2	16%, and R = 0.25	52,940
B	156.8	12%, and R = 0.38	2,310,560
C	117.6	10%, and R = 0.50	11,446,200

[1] Maximum stress applied, where $\sigma_{av} = (\sigma_{max} + \sigma_{min})/2$ is the average stress (MPa) and σ_U is UTS.
[2] Number of cycles to failure.

shown in Equation (5) for the log of the number of cycles, N:

$$\log(N) = 2.588 \left(\frac{\sigma_U}{\sigma_{max}} \right)^{0.582} \qquad [5]$$

where σ_U is the UTS (MPa) and σ_{max} the maximum stress applied (MPa). In the present study σ_U was much higher, at 921 MPa. When this value was substituted into the above equation, the expected and real values varied very significantly (Table 3).

The experimental data found here fitted the following regression equation:

$$\log(N) = 2.06 \left(\frac{\sigma_U}{\sigma_{max}} \right)^{0.6063} \qquad [6]$$

which yielded a R^2 of 0.9294.

Strain analysis and typologies

The tests showed that when the samples were tensile stressed under dynamic loads, they were progressively deformed until they failed. Strain, ε, depended on the maximum stress, σ_{max}, applied in the fatigue test. The stress-strain diagram, defined as ε *versus* N_v, is shown in Figure 4a. The curve comprises four points and three regions: P_0 represents the start conditions; P_i is the first steady state point; P_C is the critical point; and P the rupture or failure point.

The strain at the beginning of the test was undefined because steady state conditions cannot be attained in the wholly hydraulic testing frame until after a certain amount of time lapses. The σ_{max} and σ_{min} values established during this initial delay were used to determine ε_i and N_i. These coordinates in turn defined the initial

Table 3. Test of the Vázquez *et al.* (1998) model

	σ_{max} (MPa)[1]	N tested[2] (cycles)	N expected[2] (cycles)	Difference	CV[3]
A	235.2	52,940	534,302	481,362	909
B	156.8	2,310,560	17,874,616	15,564,056	674
C	117.6	11,446,200	375,021,353	363,575,153	3,176

[1] Maximum stress applied. [2] Number of cycles to failure. [3] Coefficient of variation.
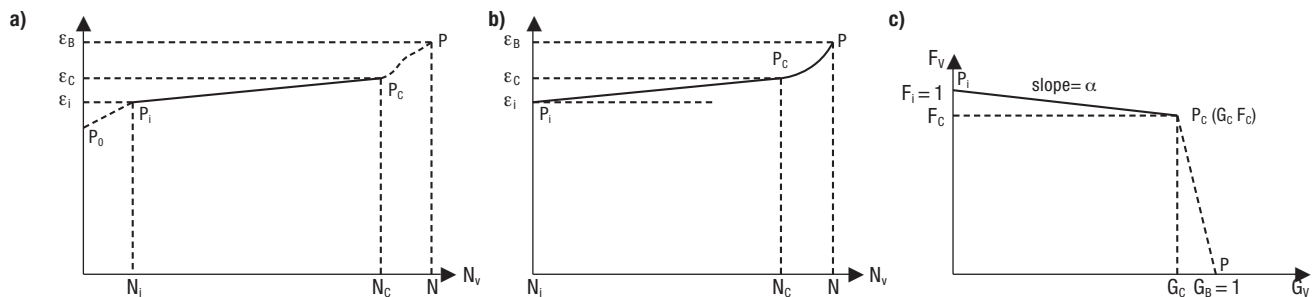
Figure 4. a) Strain (ε) *vs.* number of cycles (N_v): general pattern. b) Strain (ε) *vs.* number of cycles for type I strain. c) F_V *vs.* life factor, G_V for type I strain diagram. P_0, start point on the strain diagram; P_i, strain test start point; P_C, critical point (initial degradation of the elastic modulus); P, failure point; ε_B, strain at failure: ε_C, critical strain (at N_C); ε_i, initial strain (at N_i); $F_i = \varepsilon_i/\varepsilon_i = 1$, strain factor at the initial point; $F_C = \varepsilon_i/\varepsilon_C$, strain factor at the critical point; $G_C = N_C/N$, life factor at the critical point; $G_B = N/N = 1$, life factor at failure; α, slope of the straight line $P_i P_C$.

steady state conditions (P_i). Strain analysis was conducted between P_i and failure (Fig. 4b).

The findings revealed four strain and failure patterns. The general behaviour described in Figure 4b, observed in 72% of the samples, was defined as type I and characterized as follows:

$$\varepsilon_i < \varepsilon_C \, , \, F_C < 1 \, , \, N_C < N \, , \, G_C < 1$$

Type II behaviour, observed in 12% of the cases, was defined as:

$$\varepsilon_i < \varepsilon_C \, , \, F_C < 1 \, , \, N_C = N \, , \, G_C = 1$$

Type III behaviour was observed in 13.3% of the cases, and expressed as:

$$\varepsilon_i = \varepsilon_C \, , \, F_C = 1 \, , \, N_C < N \, , \, G_C < 1$$

Lastly, 2.7% of the cases exhibited type IV behaviour, namely:

$$\varepsilon_i = \varepsilon_C \, , \, F_C = 1 \, , \, N_C = N \, , \, G_C = 1$$

The most frequent behaviour encountered was type I. Abrupt and consequently hazardous failure of the critical region of a machine part can be prevented on the grounds of this behaviour if it is subjected to continuous monitoring and replaced when ε_i approaches ε_C. But this is not possible in 28% of the cases. The use of type I failure criteria, then, ensures safe design, particularly if useful life is defined to be N_C. Moreover, dynamic testing in which ε is not measured is an unsuitable basis for accurate and safe machine part design.

Where the only available test data exclude measurements, life expectancy (N) must be lowered by multiplying N by the respective value of G to determine the «real» life expectancy.

Table 4. Representative points on the strain diagram

Factor	P_i[1]	PC[2]	P[3]
F_v[4]$= \varepsilon_i/\varepsilon$	$F_i = 1$	$F_C = \varepsilon_i/\varepsilon_C$	$F_B = 0$
G_v[5]$= N_V/N$	$G_i = 0$	$G_C = N_C/N$	$G_B = 1$

[1] Initial point. [2] Critical point. [3] Failure point. [4] Generic strain factor at N_V cycles. [5] Generic life factor at N_V cycles.

Strain modelling as F_v versus G_v

The present study assumes type I behaviour. The stress-strain diagram in Figure 4c shows the variation in F_v with G_v. The points that define this diagram are: initial point P_i, critical point P_C, and rupture or failure point P (Table 4).

F_C and G_C are the limit values for these factors, while the straight line in the P_i-P_C region of the diagram represents the behaviour of the material. When specifically developed for F and G it adopts the following form:

$$F_V = \alpha \, G_v + 1 \qquad [7]$$

where α is the slope of the straight line (Fig. 4c) and G_v is the life factor (for N_v number of cycles). This model can be used to study the effect of load state on fatigue-induced deformation.

Table 5 gives the F_C, G_C and α values for the three series of samples. The following regression equations were obtained for F_v *vs* G_v (Fig. 5):
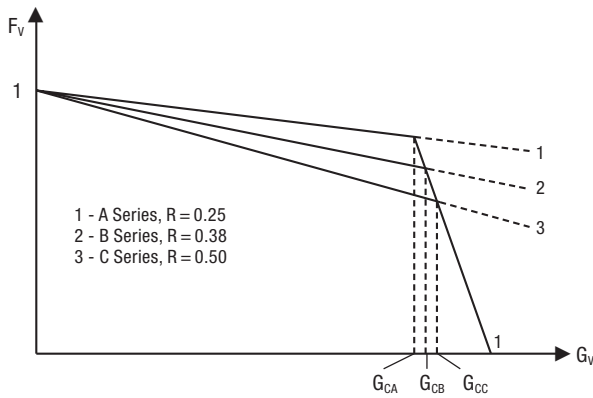
Series A:

$$F_v = -4.01 \; 10^{-2} \, G_v + 1 \qquad [8]$$

Series B:

$$F_v = -1.07 \; 10^{-1} \, G_v + 1 \qquad [9]$$

Table 5. Statistical analysis for series A, B and C

Series	Variable	CDF[4]	Characteristic value	K-S[5]
A	F_C[1]	Lognorm.	0.9665	0.9471
R = 0.25	G_C[2]	Weibull	0.9426	0.5034
	α[3]	Weibull	−0.0401	0.8852
B	F_C[1]	Weibull	0.9249	0.9365
R = 0.38	G_C[2]	Weibull	0.9665	0.8378
	α[3]	Lognorm.	−0.10695	0.9989
C	F_C[1]	Lognorm.	0.8143	0.9950
R = 0.50	G_C[2]	Webull	0.9773	0.7932
	α[3]	Normal	−0.1919	0.9915

[1] Strain factor at the critical point. [2] Life factor at the critical point. [3] Slope of the straight line between points P_i and P_C on the stress-strain diagram. [4] Cumulative distribution function. [5] Kolmogorov-Smirnov statistic

Figure 5. Regression models for strain factor, F*v vs.* life factor, G_v for series A (stress ratio R = 0.25), B (stress ratio R = 0.38) and C (stress ratio R=0.50). G_{CA}, life factor; N_C/N, for series A; G_{CB}, life factor; N_C/N, for series B; G_{CC}, life factor, N_C/N, for series C.

Series C:

$$F_v = -1.91\ 10^{-1}\ G_v + 1 \qquad [10]$$

Influence of the stress ratio R in the strain process

The data in Table 5 show that the F_C, G_C and α values varied with the stress ratio. Analysis of variance, ANOVA, findings for the mean F_C, G_C and α values for the three series revealed significant differences ($p < 0.001$), confirming that R clearly impacted the values of these variables.

Modelling N_c versus σ_{max}

If N_C is to be taken as the «useful life», a mathematical model must be developed to calculate N_C from σ_{max}. The relationship between G_C and σ_{max} was defined by conducting a regression analysis on the data in Tables 2 and 5.

$$G_C = 1.012 - 2.964\ 10^{-4}\ \sigma_{max} \qquad [11]$$

where σ_{max} is the maximum stress applied (MPa). The coefficient of correlation was $R^2 = 0.997$.

Knowing that $G_C = N_C/N$ and substituting accordingly yields:

$$N_C = \left(1.012 - 2.964\ 10^{-4}\ \sigma_{max}\right) 10^{\left(\frac{471.74 - \sigma_{max}}{49.91}\right)} \qquad [12]$$

Modelling expected life for a maximum value of strain

Some machine parts, subjected to dynamic loads, cannot work properly and safely if deformed beyond a certain threshold. In such cases, the «real» useful life is neither N_C nor N, but the value of N_v corresponding to the maximum design strain, F_m. The life expectancy corresponding to F_m, which is found from factor F_v, would be N_s.

The regression equation that relates α to σ_{max}, found from the data in Tables 2 and 5, is as follows:

$$\alpha = 0.032 + 1.228\ 10^{-3}\ \sigma_{max} \qquad [13]$$

The correlation coefficient was $R^2 = 0.966$.
In light of Eq. [13], Eq. [7] can be rewritten as follows:

$$F_v = (0.032 + 1.228 10^{-3}\ \sigma_{max})\ G + 1 \qquad [14]$$

For the maximum admissible deformation, F_v becomes F_m and substituting G_v for N_s/N Eq. [14] becomes:

$$F_m = (0.032 + 1.228\ 10^{-3}\ \sigma_{max})\ (N_s/N) + 1 \qquad [15]$$

Finally, solving for N_s yields:

$$N_s = \frac{\left(F_m - 1\right) 10^{\left(\frac{471.74 - \sigma_{max}}{49.91}\right)}}{0.032 + 1.228\ 10^{-3}\ \sigma_{max}} \qquad [16]$$

When $F_m = F_C$ (see Table 5), the characteristics values of N (Tables 2 and 6) for series A, B, C, 2H and 3H were very highly correlated ($R^2 = 0.99$) to the data obtained with Eq. [16].

Moisture effect

The study included one set of control samples not exposed to ageing, one set exposed to two wet/dry cycles (2H) and one to three such cycles (3H). As the mechanical findings given in Table 6 show, no significant differences were observed in any of the properties compared. In other words, moisture had no effect on fatigue strength, for the mean life of samples subjected to accelerated ageing was no lower than mean life of the control samples.

Discussion

Static tests

While the composite material studied exhibited essentially brittle behaviour, two linear regions were

Table 6. Typical values for series B (without ageing), 2H and 3H

Variable	Series B	Series 2H	Series 3H
σ_{max}[1]	156.8	156.8	156.8
Load state	12% UTS, R = 0.38	12% UTS, R = 0.38	12% UTS, R = 0.38
Number of tests	12	12	11
ε_i[2]	1.661A-03	1.760E-03	1.630E-03
N_C (cycles)[3]	1,715,210	1,705,830	1,618,140
N (cycles)[4]	1,806,040	1,747,200	1,688,230
F_C[5]	0.9249	0.9086	0.8948
G_C[6]	0.9663	0.9794	0.9743
α[7]	−1.070E-01	−1.223E-01	−1.538E-01

[1] Maximum stress applied. [2] Initial strain. [3] Number of cycles at the critical point. [4] Number of cycles at failure. [5] Strain factor at the critical point. [6] Life factor at the critical point. [7] Slope of the straight line between points P_i and P_C on the stress-strain diagram.

observed on the tensile stress-strain diagram. The ultimate tensile strength, yield stress and elastic modulus of all the samples tested followed Weibull normal and lognormal CDFs. No correlation was found between volume percentage of fibre and material UTS.

Dynamic tests (life)

Cyclical loads ranging from 10 to 16% of the UTS gave life expectancy values of ten thousand to ten million cycles.

The results for the new GFRP tested did not fit the multiplicative model obtained previously for a similar GFRP. Consequently, the model must be re-established for every GFRP.

The present findings indicate that the multiplicative model is suitable to predict GFRP useful life under sinusoidal loads. Since the model coefficients vary with the type of GFRP, however, each material must be tested separately. Nonetheless, since exponent values were very similar in the two models, similar GFRPs may be expected to have essentially the same exponent, although more experiments would obviously be required to confirm this hypothesis.

Dynamic test (strain)

The proposed deformation diagram, whose general pattern is depicted in Figure 4a, represents the variation in linear deformation, ε, over the life of the specimen subjected to fatigue.

In 72% of all the tests conducted, which covered a majority of the samples assessed (other authors, such as Bach (1994), have reported similar findings), the stress-strain diagram showed that critical strain, ε_C, was higher than the initial strain, ε_i. At the same time, the number of fatigue cycles prior to reaching the critical point, N_C, was consistently lower than the number of cycles required for specimen failure, N. The maximum strain value and number of fatigue cycles at the critical point constitute very useful information for structural part design.

The life factors ($G_C = N_C/N$) in Table 5 show that the useful life of samples, N_C, came to 94, 96 and 97% of the failure life for 10^4, 10^6, and 10^7 fatigue cycles, respectively.

The characteristic values obtained for strain factor F_C showed that initial strain, ε_i, was 96, 92 and 81% of the critical strain, ε_C, for 10^4, 10^6, and 10^7 fatigue cycles, respectively. «In situ» measuring of strain factor F_C is useful for deciding when structural elements should be replaced.

Influence of stress ratio R

The data in Table 5 show that F_C declines with rising R and that. Similarly, the growth in the rate of strain, α, and the life factor, Gc, with rising R entails a shortening of the time lapsing between the critical and failure points.

Nonetheless, a special program of tests would have to be run to obtain more values of R and confirm its effect on factors Fc and G_C. If R is found to have no effect on GFRP life expectancy (Vázquez *et al.,* 1998) and the effect of R on strain is confirmed, the conclusion would be that the failure point for a given σ_{max} would be the same for different strain processes,
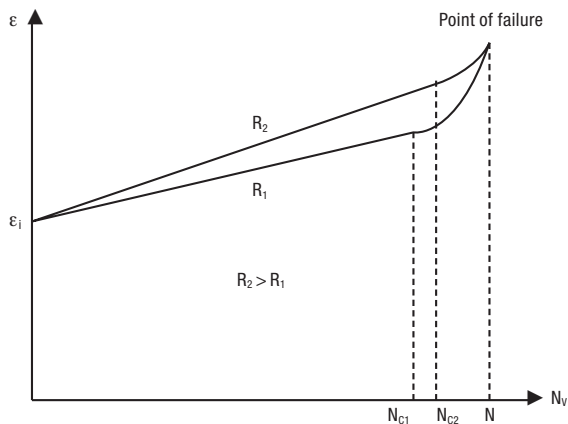
Figure 6. Strain, ε, *vs.* number of cycles, N. Theoretical curve, showing the effect of R on strain and fatigue failure. ε_i, initial strain (at N_i); N_{C1}, number of cycles at the critical point for stress ratio R_1; N_{C2}, number of cycles at the critical point for stress ratio R_2; N, number of cycles at failure.

depending on R. Confirmation of this hypothesis (shown in Fig. 6) is of utmost importance, for a substantial number of machine parts (including wind turbine blades), are designed to work at a pre-set ε value.

Influence of the cycle of ageing (moistening/drying at room temperature)

Under humid conditions, the resin in the GFRP absorbs water, which spreads across the fabric to the matrix-fibre interface (Gerharz and Schütz, 1980). This first de-stabilises the material and subsequently exposes the fibres to possible oxidation-induced deterioration. Water fills and widens cracks, accelerating the propagation of water molecules throughout the material and the concomitant degradation. According to Wang and Wang (1980), a glass and polyester material's fatigue resistance depends on the water diffusion rate in the matrix and the direction of the fibres. Similarly, Hull (1987) reported that the resin in composite materials acts like a semi-permeable membrane. Consequently, when they are subjected to fatigue, the osmotic pressure exerted by water can lead to crack propagation.

Other authors (Gitschner and Menges, 1979) conducted accelerated hot water immersion tests.

Moisture-induced degradation is seldom totally reversible because the material fails to recover its initial mechanical properties (Scola, 1975).

In this study, ageing (see Fig. 7) was found to have no significant effect on material fatigue strength or strain. Other authors, however, such as Watanabe (1979), reported a sizeable decline in fatigue strength in a test sample immersed in water. In samples wetted and dried, he found no reduction in fatigue strength prior to 10^7 cycles, although at higher numbers he observed declines of 7%. Working with polyester glass, Boller (1969) observed an abrupt slide in fatigue strength in moist air for small numbers of cycles. He also found a 10% reduction in expected life in large numbers of cycles ($< 10^7$), but no reduction in this variable for very large numbers of cycles ($> 10^7$).

Bach (1993, 1996) immersed a GFRP material in water at 50°C for 14 days and subsequently tested it at 100% relative humidity. The water content reached 0.13% by weight during this process. The moisture absorbed reduced ultimate tensile strength by 15% and fatigue strength by 35% (through 1,000 cycles) and 10% (through 10^7 cycles). Vázquez *et al.* (1998) submerged samples in water at ambient temperature (24°C) for 45 days. The tests were conducted at laboratory temperature, *i.e.,* 25°C. The samples, with a mean water content of 0.15 to 0.20%, were tested under a load of 30% of UTS and R = 0.4. Their findings showed that moisture had no clear effect on tensile strength prior to 10^5 cycles.
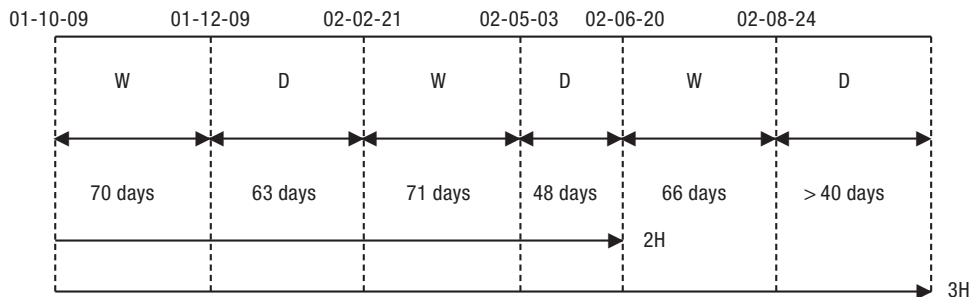
Figure 7. Ageing treatment timetable for samples subjected to two (2H) or three (3H) wet-dry cycles. W: inmersión in water 20°C. D: drying in environmental conditions.

Acknowledgements

References

ANDERSEN S.L., LILHOT H., 1988. Fatigue of glass/polyester composite materials for wingblades. European Community Wind Energy Conference, Herning, Denmark, 6-10 June, pp. 324-346.

ANDERSON, 1996. Properties of composites with long fibres. In: Design of composite structures against fatigue (Mayer R.M., ed). John Wiley and Sons Ltd, Denmark.

BACH P.W., 1988. High cycle fatigue investigation on windturbine materials. Proceedings of European Community Wind Energy Conference, Herning, Denmark, 6-10 June, pp. 337-341.

BACH P.W., 1991. High cycle fatigue testing of glass fibre reinforced polyester and welded structural details. Report ECN-C-91-010. Netherlands Research Energy Foundation, Petten, The Netherlands.

BACH P.W., 1992. Fatigue properties and design of wing blades for windturbines. Joule Project, Progress Report. pp. 250-251.

BACH P.W., 1993. The effect of moisture of the fatigue performance of glass fibre reinforced polyester coupons and bolted joints. European Community Wind Energy Conference, Lübeck-Travemünde, Germany. pp. 180-183.

BACH P.W., 1994. Fatigue lifetime of glass polyester laminates for wind turbine blades. Report ECN-C-94-020. Netherlands Research Energy Foundation, Petten, The Netherlands.

BACH P.W., 1996. The effect of moisture of the fatigue performance of glass fibre reinforced polyester coupons and bolted joints. Report ECN-C-96-015. Netherlands Research Energy Foundation, Petten, The Netherlands.

BOLLER K.H., 1969. Fatigue fundamentals for composite materials. American Society for Testing and Materials. American Society of Testing and Materials, STP 460. pp 217-235.

GERHARZ J.J., SCHÜTZ D., 1980. Literature research on the mechanical properties of fibre composite materials. Analysis of the state of the art. Royal Aircraft Establishment. Library Report. Translation 2045. Vol. 1, pp. 29-30.

GITSCHNER H.W., MENGES G., 1979. Sorption, swelling and creep behaviour of glass fibre reinforced composite materials. Conference: Recent advances in the properties and applications of thermosetting materials. Plastic & Rubber Institute. 5-6 Dec. Coventry. pp. 15.1-15.8.

GREENWOOD J., 1981. The long term stress rupture, creep and fatigue properties of glass reinforced polyester and epoxide resin: introduction to the literature survey. ERA report No. 81-120R. Project No. 71/01/3713.

HULL D., 1987. Materiales compuestos. Ed Reverté, Barcelona. [In Spanish].

HWANG W., HAN K.S., 1986. Fatigue of composite-fatigue modulus concept and life prediction. J Composite Material 24, 125-165.

MANDELL J.F., 1982. Development in reinforced plastics. Vol 2 (Pritchard O., ed). Applied Science Publishers, London. 67 pp.

O'BRIEN T.K., 1985. Analysis of local delaminations and their influence on composite laminate behaviour. American Society for Testing and Materials.

OLLER S., 2002. Análisis y cálculo de estructuras de materiales compuestos. Universidad Politécnica de Cataluña, Barcelona. [In Spanish].

PARIS P.M., GÓMEZ M., ANDERSON W., 1961. A rational analytic theory of fatigue. The Trend in Engineering 13, 9-14.

REIFSNIDER K.L., 1991. Fatigue of composite materials. Elsevier, Amsterdam.

SCOLA D.A., 1975. A study to determine the mechanisms of S-glass/epoxy resin composite degradation due to moist and solvent environment. Proc Annual Conference – Reinforced Plastics/Composites Institute, Society of the Plastics Industry, NY, 30, 19.

TALREJA R., 1986. Fatigue of composite materials. Technomic Publ. Inc, Lancaster, PA, USA.

TALREJA R., 1997. A damage mechanics based approach to durability assessment of composite material. In: Composites and functionally graded materials, MD-Vol 80. American Society of Mechanical Engineers. pp. 151-156.

VÁZQUEZ J., SILVERA A., ARIAS F., SORIA E., 1998. Fatigue properties of a glass-fibre-reinforced polyester material used in wind turbine blades. J Strain Anal Eng 33(3), 183-193.

WANG C.S., WANG A.S., 1980. Creep behaviour of glass-epoxy composite laminates under hygrothermal conditions. In: Advances in composite materials (Bunsell *et al.*, ed). Vol. 1. Pergamon Press, Paris. pp. 569-578

WATANABE M., 1979. Effect of water environment on fatigue behaviour of fibre reinforced plastic . Proc 5th Conference on Composite Materials, Testing and Design, ASTM STP 674, Philadelphia, PA, USA. pp. 345-367.

YANG J., DU S., 1983. An exploratory study into the fatigue of composites under spectrum loading. J Comp Mater 17, 511-526.